Computational Chemistry Workshops
West Ridge Research Building-UAF Campus
9:00am-4:00pm, Room 009

Electronic Structure - July 19-21, 2016
Molecular Dynamics - July 26-28, 2016

Computational Coordination Chemistry

Introduction

The rich chemistry of transition metals gives rise to the large and important fields of coordination chemistry, organometallic chemistry and branches of solid state chemistry. In fact, transition metal complexes play an important role in biology and chemical catalysis, since they are able to catalyze a very large variety of reactions, many of them of fundamental relevance to biological and industrial processes. The high reactivity of transition metal complexes is intimately linked to their electronic structure and the nature of the metal-ligand bonds. In fact, metal-ligand bonds are reasonably strong, but are weaker than the typical covalent bonds formed in organic chemistry. Consequently, the metal-ligand bonds are easier to break and reform which gives rise to low-energy pathways in chemical reactions.

Because of partially filled d-shells, most of the transition metals are redox active and can exist in different oxidation states (e.g. Mn can assume oxidation states: -I, 0 - VII). The potential at which the one-electron steps occur is a sensitive function of the nature of the ligands and the coordination geometry which, therefore, can be easily tuned by suitable ligand design. In addition, the partially filled d-shells of transition metals contain unpaired electrons which gives rise to several accessible spin states and may show considerably different reactivities, leading to added complexity in studying their reactions. Frequently, the systems may pass from one spin state to another surface during a given catalytic cycle, opening many fascinating routes to unique reactions.

Lastly, the partially filled d-shells, and the variable metal-ligand bonds, are associated with a huge variety of fascinating spectroscopic phenomena. Thus, very detailed insight into the geometric and electronic structure of the transition metal sites can be obtained from spectroscopic studies, which frequently yield the key to understanding the unique reactivities displayed by transition metal complexes.

Goals of Exercises

In these exercises, basic aspects of coordination chemistry will be studied, by combining the use of Ligand Field Theory (LFT) as a conceptual framework and Molecular Orbital calculations to successfully interpret experimental results.

Ligand Field Theory

Beyond all advanced theoretical considerations, the major driving force for the formation of coordination complexes is the electrostatic attraction of a positively charged metal ion and a negatively charged ligand or a ligand with functional groups that bear a partial negative charge, and shown schematically in Figure 1, from the computed electrostatic potential of the typical ligand ehthylenediamine.

Traditionally, the properties of such coordination compounds are interepreted in the framework of a theory that was worked out in the 1950s by physicists (mainly Hans Bethe) and

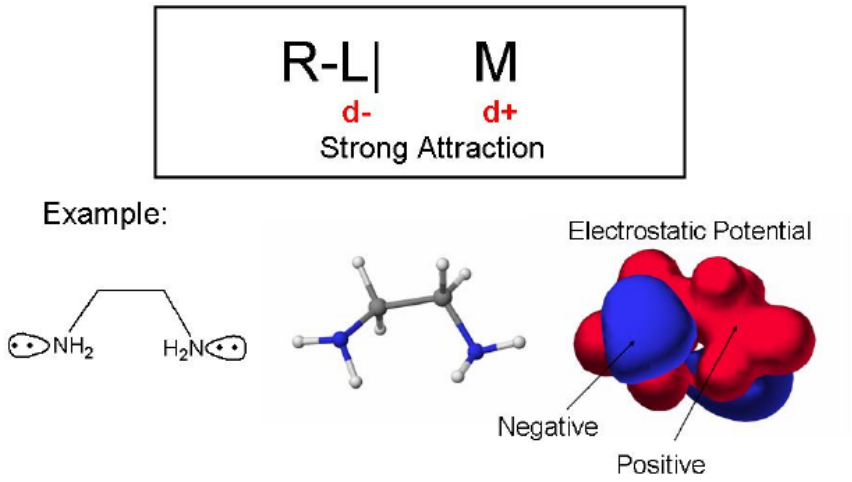

Figure 1: Schematic Reaction Showing the Formation of a Coordination Compound

is called crystal field theory. Slightly more chemistry oriented modifications are known collectively as Ligand Field Theory, but these terms will not be differentiated. The essential idea is to focus interest on the open d-shells of the metals and study their interaction with their environment which is assumed to somehow provide an electrostatic field in which the d-electrons have to move.

Thus, LFT does not involve a detailed account of chemical bonding, but is enormously successful in its domain of applicability. In fact, using LFT many properties of large classes of complexes can be understood in a unified and simple language. In particular, the concept of a d^n-metal (n=number of d-electrons) that is so central to inorganic chemistry would not be possible without LFT. The concepts are usually worked out on the example of octahedral coordination complexes. While exactly octahedral complexes are rather rare, approximately octahedral complexes are highly abundant and the conclusions drawn from studying the octahedral case largely remain valid.

The shapes of the d-orbitals are well known and are shown in Figure 2. The ligands are assumed to be placed along the axes of the coordinate system such that an octahedral field of negative point charges arises. This set of negative point charges now starts to interaction with a probe electron that is placed into each of the five d-orbitals in turn. Upon evaluating the energy of interaction of the probe electron with the negative point charges it is found that the energy is different for the different orbitals as shown in Figure 3.

As a consequence of lowering the symmetry of the surrounding free ion from spherical to octahedral symmetry in the transition metal complex, the degeneracy of the five d-orbitals is lifted. In fact, from Figure 3 an electron that occupied the $d_{x^2-y^2}$, or the d_{z^2} orbital may be, on average, more strongly repelled by the negatively charged ligand than an electron that occupied the d_{xy}, d_{xz}, or d_{yz} orbitals. A quantitative treatment, based on group theory, shows that the set of five d-orbitals fall into a t_{2g} subshell at lower energy, and an e_g shell at higher energy. The classic and rigorous mathematical textbook by J.S. Griffith, *The Theory of Transition-Metal Ions*, Cambridge University Press, Cambridge, 1964. has many insights

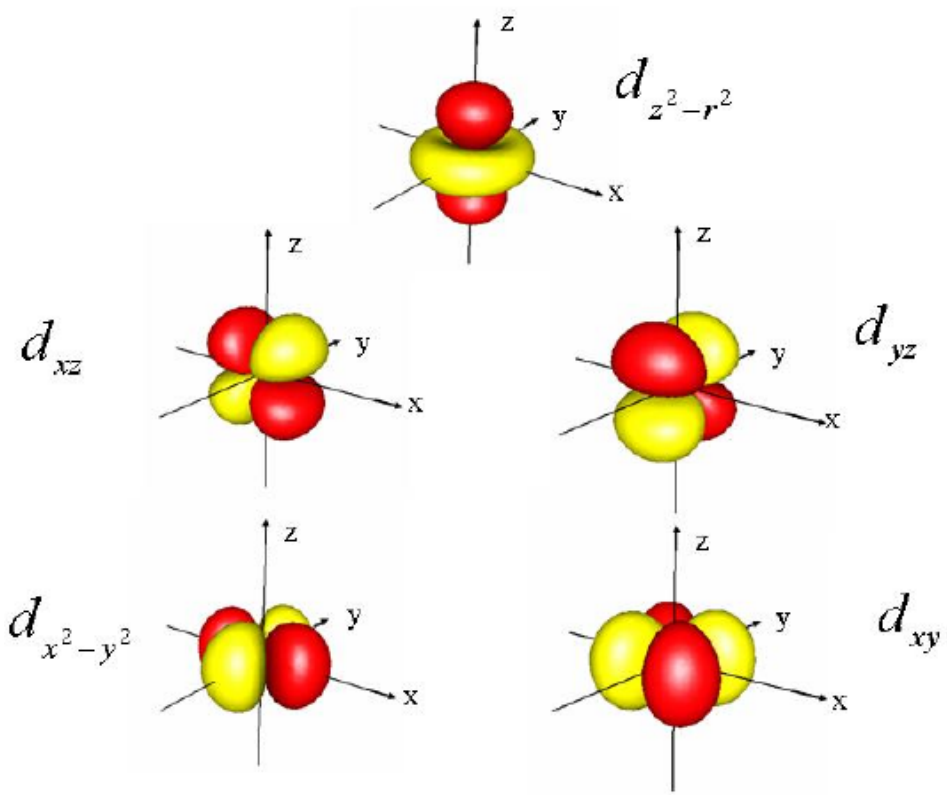

Figure 2: Shapes of the five d-orbitals together with their common designation in terms of real spherical harmonics. The combination $z^2 - r^2$ is usually only abbreviated as z^2.

that rigorously carry over to the modern methods of Quantum Chemistry. A thorough understanding of Ligand Field Theory can teach us an enormous amount about the N-electron problem in Quantum Chemistry.

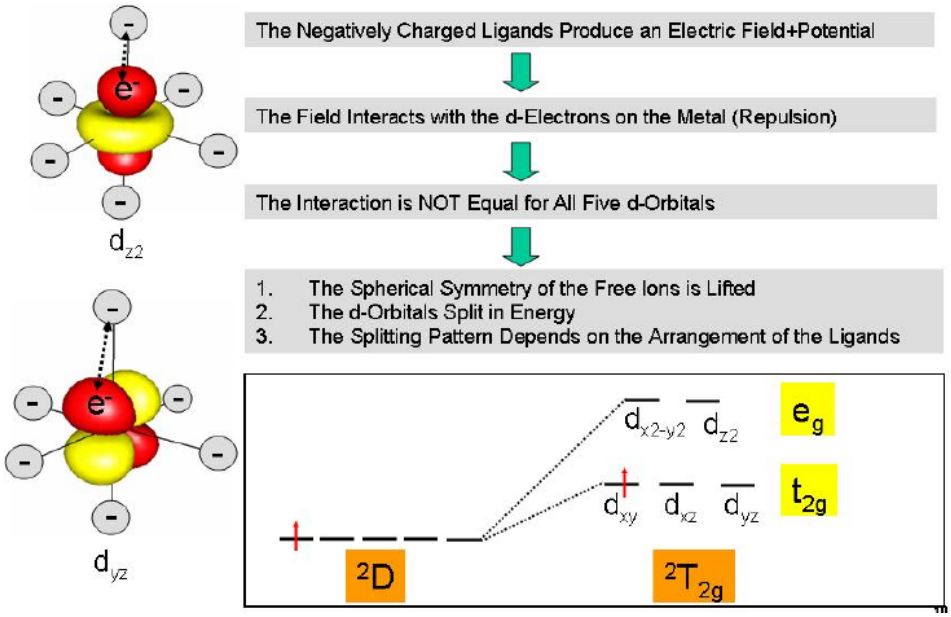

Figure 3: d-Orbital Splittings induced by an octahedral ligand field.

Note carefully, that these energies are not drawn to scale. Above all, the repulsion leads to a strong increase of the energies of all five d-orbitals and the relatively small difference in the energy increase is the ligand-field splitting. Note also, that the final result does not depend on how the coordinate system is placed. Thus, the result is said to be rotationally invariant. What does change, if the coordinate system is rotated, is the designation of the orbitals.

Capital letters refer to many electron states, and lowercase letters to one-electron orbitals. Furthermore, the term symbol carries the total multiplicity as a left superscript, $2S + 1$, of the state, where S is the total spin of this state.

Following the rules of how to assign the many electron term symbol from the one-electron MO scheme, it is evident that the configuration $(t_{2g})^1(eg)^0$ gives rise to a ${}^2T_{2g}$ term, while the higher energy configuration $(t_{2g})^0(e_g)^1$ gives rise to an ${}^2E_g$ term in O_h symmetry. Since the T irreducible representation is three-dimensional, and the E representation is two-dimensional, the ${}^2T_{2g}$ is threefold orbitally degenerate, and ${}^2E_g$ is two-fold orbitally degenerate. The total degeneracy of the state in the absence of spin-orbit coupling (SOC) and magnetic fields is $2S + 1$ times the orbital degeneracy which amounts to six for ${}^2T_{2g}$ and four for ${}^2E_g$ for the present case.

All of these ten states are observable and can be probed by spectroscopic experiments. One of the simplest experiments is to induce a ${}^2T_{2g} \rightarrow {}^2E_g$ transition, by application of a visible photon of suitable energy. The experiment provides a quantitative measure of the d-orbital splitting, Δ_0, which is typically in the range 1-4 eV (8000-32000 cm^{-1}). The example of $[Ti(H_2O)_6]^{3+}$ in Figure 4 shows that this is a slight over simplification, since a broad and asymmetric absorption band is observed, rather than a single line like in atomic spectroscopy.

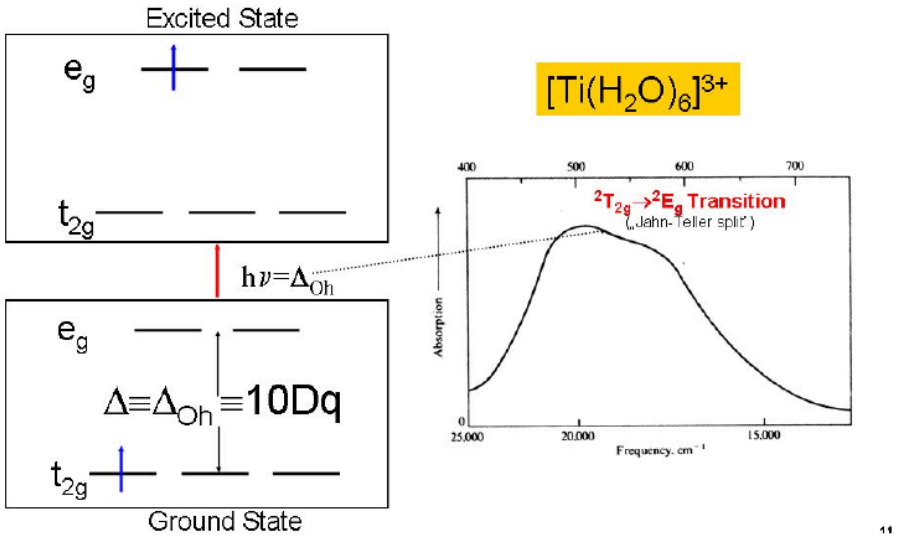

Figure 4: Example of the measurement of the ligand field splitting in $[\mathrm{Ti}(\mathrm{H_2O})_6]^{3+}$

However, we will not go into any further detail of the interpretation of the spectrum here but merely assume that it is possible extract reasonable values of the ligand field splitting Δ_0 from the study of the absorption spectra of the complexes. Since the magnitude of the splitting depends on the nature of the ligand, the ability of the ligand to induce d-orbital splittings may be classified in the spectrochemical series shown in Figure 5.

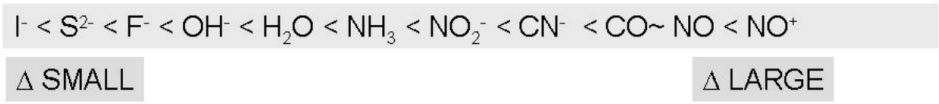

Figure 5: The spectrochemical series.

On this basis CN^- is known to be a strong-field ligand since it gives rise to large ligand field splittings and I^- is known to be a weak field ligand since it gives rise to small ligand field splittings.

Please observe an apparent irregularity: $OH^-$is a weaker field ligand than H_2O, despite the fact that it is actually negatively charged. This should not be the case if our reasoning about the origin of the ligand field splitting above is correct, and we will revisit this later.

A nice experimental confirmation that this way of thinking about the electronic structure of transiton metal complexes makes sense, is shown in Figure 6 where the experimental enthalpies of formation of $[\mathrm{M}(\mathrm{H_2O})_6]^{2+}$ complexes are shown, and M is a first row transition metal.

The interpretation of the results is as follows: The enthalpy of formation is increasing along the series. Thus, the later transiton metals hold the water ligands more strongly than the early transition metals. This is, first of all, an effect of the effective nuclear charge of the metal. Since the *d*-electrons shield the increasing nuclear charge with increasing atomic

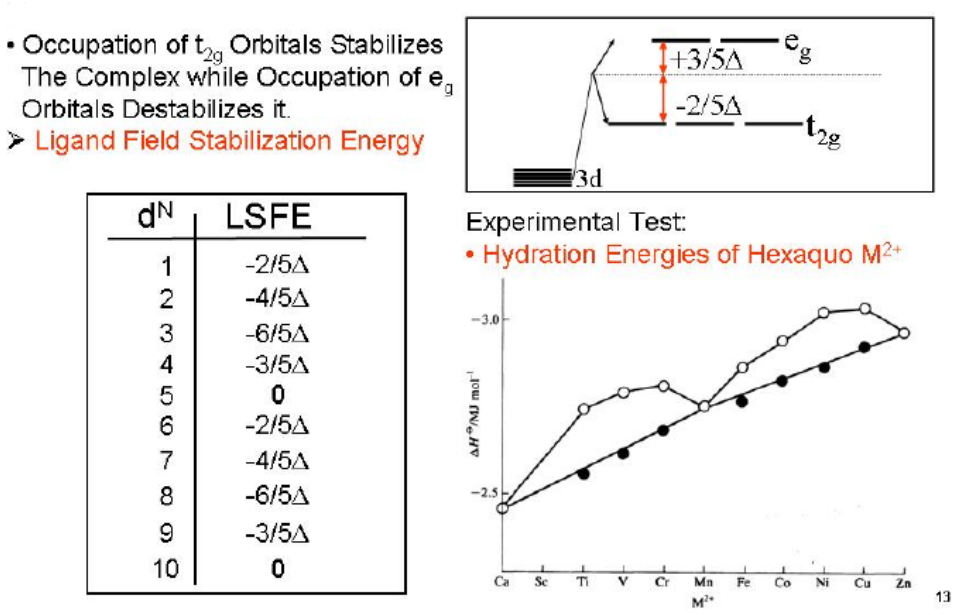

Figure 6: Thermochemical confirmation of ligand field splittings: the Ligand Field Stabilization Energy (LFSE). The enthalpies of formation are plotted for the hexaquo complexes for the divalent first-row transition metal ions. Open circles designate raw experimental data, while full circles signify subtraction of the LSFE.

number less effectively, the ligands see an increased positive charge from the metal which leads to the slope of the line. However, more interestingly is the double-bowl behavior of the experimental data. This readily finds an explanation from considering the energy of a given d^n configuration relative to the hypothetical case where all d-orbitals have the same energy: thus occupation of a t_{2g} level leads, on average, to an energy decrease of - $2/5\Delta_0$ while occupation of an e_g level leads to a $3/5\Delta_0$ increase. Knowing the Δ_0-values from optical spectroscopy, the LFSE of a given d^n configuration can be subtracted from the experimental data to arrive at the full circles which now perfectly fall on a straight line. Thus, in this way, one has found a simple explanation for a seemingly puzzling and irregular experimental result.

Electron-Electron Repulsion Effects

A little thought shows that our discussion of the energies of d^n configurations is somewhat over simplified, since electrons are negatively charged and repel each other, but has not yet been taken into account. As mentioned in the introduction, the electron-electron repulsion is the biggest challenge for theoretical chemistry. The accurate calculation of electron correlation from physical principles is very difficult and represents a major branch of research in Quantum Chemistry.

Electron-electron repulsion leads to a number of important effects in coordination chemistry. First of all, two rules-of-thumb should be mentioned: (a) electrons that occupy the same

orbital repel each other most strongly, and (b) electrons of opposite spin repel each other more strongly than electrons of the same spin. Thus, the system will want to assume the configuration where as much as possible the electrons have the same spin and occupy different orbitals. This leads to multiplet splittings for d^n configurations where states of different multiplicity but the same electron configuration have different energies.

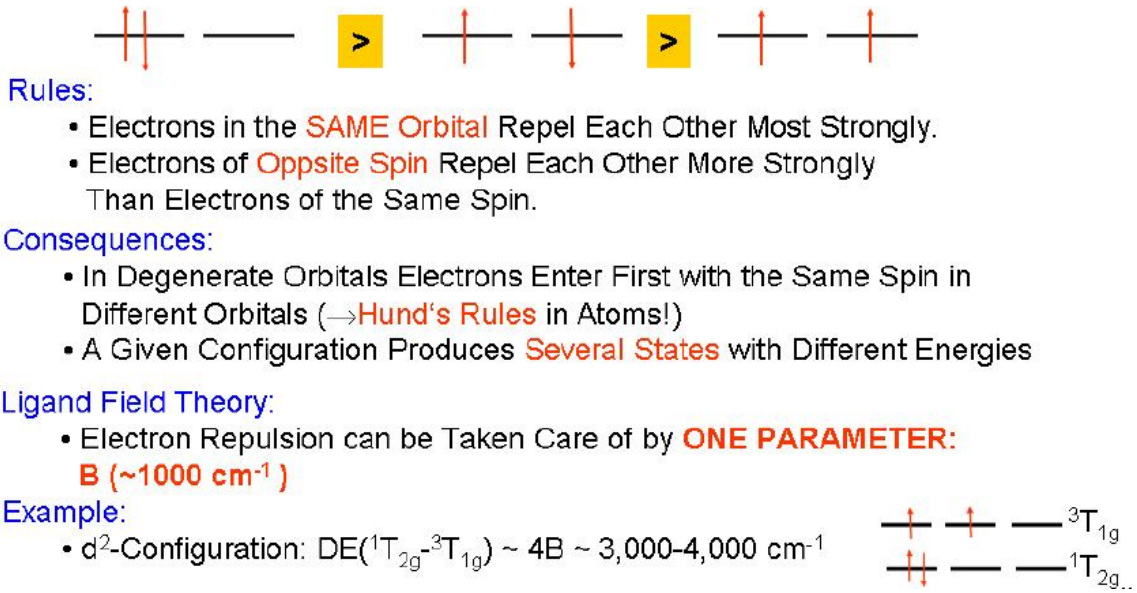

Figure 7: Principles of electron-electron repulsion in LFT.

In LFT, one has the fortunate situation that electron-electron repulsion can be described to a good approximation with a single parameter: the Racah B-value. Thus, besides the ligand-field splitting parameter Δ_0, the second important parameter of LFT is the B-value, which is of the order of $\sim$1000 cm^{-1}, and yields state splittings are typically multiples of B. The example in Figure 7 is the $^1T_{1g} - {}^3T_{2g}$ splitting (both derived from the $(t_{2g})^2(e_g)^0$ configuration) is 4B and experimentally the splitting between these states is 3000-4000 cm^{-1}.

The electron-electron repulsion has a very interesting consequence: for several of the d^n configurations (actually $d^4 - d^7$), it is not a priori clear which electron configuration will be of lowest energy since there is a competition between ligand-field splitting and electron-electron repulsion (Figure 8).

For example, for the case of the d^5 configuration, the high-spin state ($(t_{2g})^3(e_g)^2$; $^6A_{1g}$) minimizes the electron-electron repulsion according to our rules-of-thumb, but at the expense of promoting two electrons into the higher-energy e_g-orbitals. This can be avoided by forming the alternative low-spin ($(t_{2g})^5(e_g)^0$; $^2T_{2g}$) configuration which maximizes the LSFE, but at the expense of a larger electron-electron repulsion. Thus, depending on the ligand environment either one, or the other alternative, will be preferred: strong field ligands lead to low-spin complexes and weak field ligands to high-spin complexes. Experimentally, this is found to be true: $[Fe(CN)_6]^{3-}$ has a $^2T_{2g}$ ground state, while $[FeCl_6]^{3-}$ has a $^6A_{1g}$ ground state.

Everything that has been said about the nature of the two dominating influences: ligand

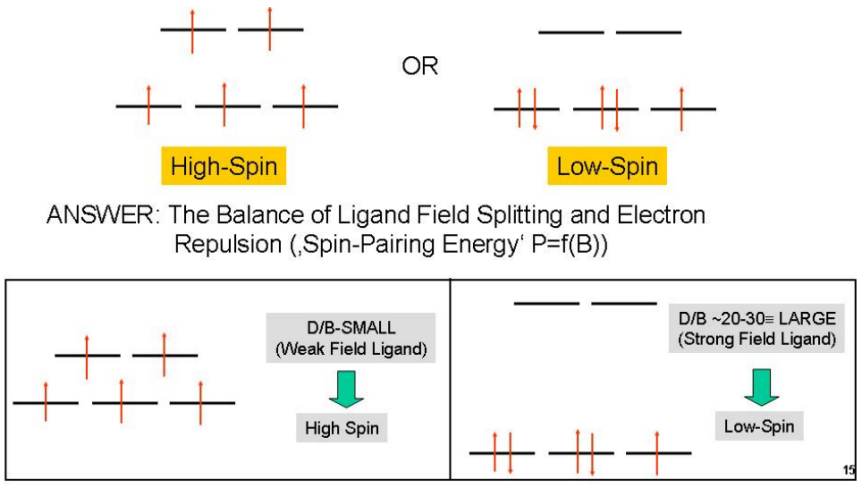

Figure 8: Competition between electron-electron repulsion and ligand field splitting to produce either high-spin or low-spin complexes.

field splitting and electron-electron repulsion can be nicely summarized and systematized in the so-called Tanabe-Sugano diagrams (Figure 9). What is plotted there on the x-axis is the ligand field strength in units of B while on the y-axis the energy of a given state relative to the lowest state of the system is plotted.

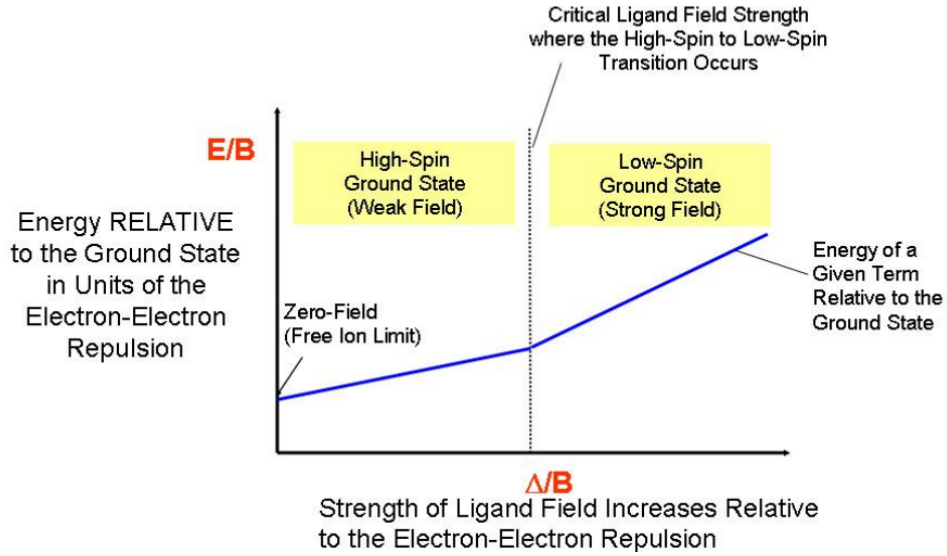

Figure 9: General organization of a Tanabe-Sugano Diagram.

For the $d^4 - d^7$ electron configurations, Tanabe-Sugano diagrams have two parts: a weak field part, where the high-spin state is the ground state and a strong field part, where the low-spin state is the ground state. At some critical ligand field strength, a discontinous change from one ground state to the other occurs. Experimentally, this is known to be possible: complexes with ligands that lead to ligand field strengths close to the crossover point are known to be switchable from one ground state to the other by external perturbation such as

pressure.

This leads to the interesting field of spin-crossover chemistry which is a promising approach to the design of molecular switches. Secondly, the Tanabe-Sugano diagrams are excellent guides to the assignment of the ligand-field absorption spectra of transiton metal complexes. Given that the selection rule, $S = 0$, for an electric dipole allowed transition between two states is fairly strong, one simply has to search in the Tanabe-Sugano diagram for states of the same multiplicity as the ground state in order to find out how many ligand-field bands are expected in the absorption spectrum.

The only thing that is needed, then, in order to determine Δ_0, is a ruler and a reasonable estimate of B. Two examples of such diagrams together with actual absorption spectra are shown in Figure 10.

The spin-allowed ligand field bands are weak, since they are parity forbidden in octahedral complexes. However, in tetrahedral complexes, there is no center of inversion, and the observed ligand field bands are much stronger than in octahedral complexes. Spin-allowed ligand field bands can have absorbtivity (ε) values that are several hundred $M^{-1}cm^{-1}$, while spin-forbidden transitions typically have absorbtivity (ε) values < 1 $M^{-1}cm^{-1}$.

A summary of the many-electron terms, together with the leading one-electron configurations. is shown in Table 1.

d^N	Ground Term O_h	Config.	Spin-Allowed Transitions	Spin-Forbidden Transitions
d^9	^2E_g	$t_{2g}^6e_g^3$	$^2T_{2g}(t_{2g}^5e_g^4)$	None
d^8	$^3A_{2g}$	$t_{2g}^6e_g^2$	$^3T_{2g}(t_{2g}^5e_g^3)$ $^3T_{1g}(t_{2g}^5e_g^3)$ $^3T_{1g}(t_{2g}^4e_g^4)$	$^1E_g(t_{2g}^6e_g^2)$ $^1T_{2g}(t_{2g}^5e_g^3)$
d^7	$^4T_{1g}$	$t_{2g}^5e_g^2$	$^4T_{2g}(t_{2g}^4e_g^3)$ $^4T_{1g}(t_{2g}^4e_g^3)$ $^4A_{2g}(t_{2g}^3e_g^4)$	$^2E_g(t_{2g}^6e_g^1)$ $^2A_{2g}(t_{2g}^5e_g^2)$ $^2T_{2g}(t_{2g}^5e_g^2)$
d^6	$^5T_{2g}$	$t_{2g}^4e_g^2$	$^5E_g(t_{2g}^3e_g^3)$	$^3T_{2g}(t_{2g}^5e_g^1)$
d^5	$^6A_{1g}$	$t_{2g}^3e_g^2$	None	$^4T_{1g}$, $^4T_{2g}$ $(t_{2g}^4e_g^1)$ $^4A_{1g}$, ^4E_g, $^4T_{2g}(t_{2g}^3e_g^2)$
d^4	^5E_g	$t_{2g}^3e_g^1$	$^5T_{2g}(t_{2g}^2e_g^2)$	$^3T_{1g}(t_{2g}^2e_g^2)$
d^3	$^4A_{2g}$	$t_{2g}^3e_g^0$	$^4T_{2g}(t_{2g}^2e_g^1)$ $^4T_{1g}(t_{2g}^2e_g^1)$ $^4T_{1g}(t_{2g}^1e_g^2)$	$^2E_g(t_{2g}^3)$ $^2T_{1g}(t_{2g}^3)$
d^2	$^3T_{1g}$	$t_{2g}^2e_g^0$	$^3T_{2g}(t_{2g}^1e_g^1)$ $^3T_{1g}(t_{2g}^1e_g^1)$	$^1E_g(t_{2g}^2)$ $^1T_{2g}(t_{2g}^2)$ $^1A_{1g}(t_{2g}^2)$
d^1	$^2T_{2g}$	$t_{2g}^1e_g^0$	$^2E_g(t_{2g}^0e_g^1)$	None

Table 1: Ground- and Excited- Ligand Field States of Octahedral d^n Complexes.

Other Coordination Geometries

The entire chain of arguments developed so far is valid only for octahedral complexes. However, in reality, coordination compounds exist in many different effective geometries with coordination numbers ranging from 2-8. Each distinct coordination geometry induces a different orbital splitting pattern and therefore also a different set of molecular multiplets. For some of the more important coordination geometries the orbital splitting patterns are shown in Figure 11.

While each of these geometries would require an elaborate analysis, it is clear that the absorption spectra of coordination complexes react very sensitively to the coordination geometry

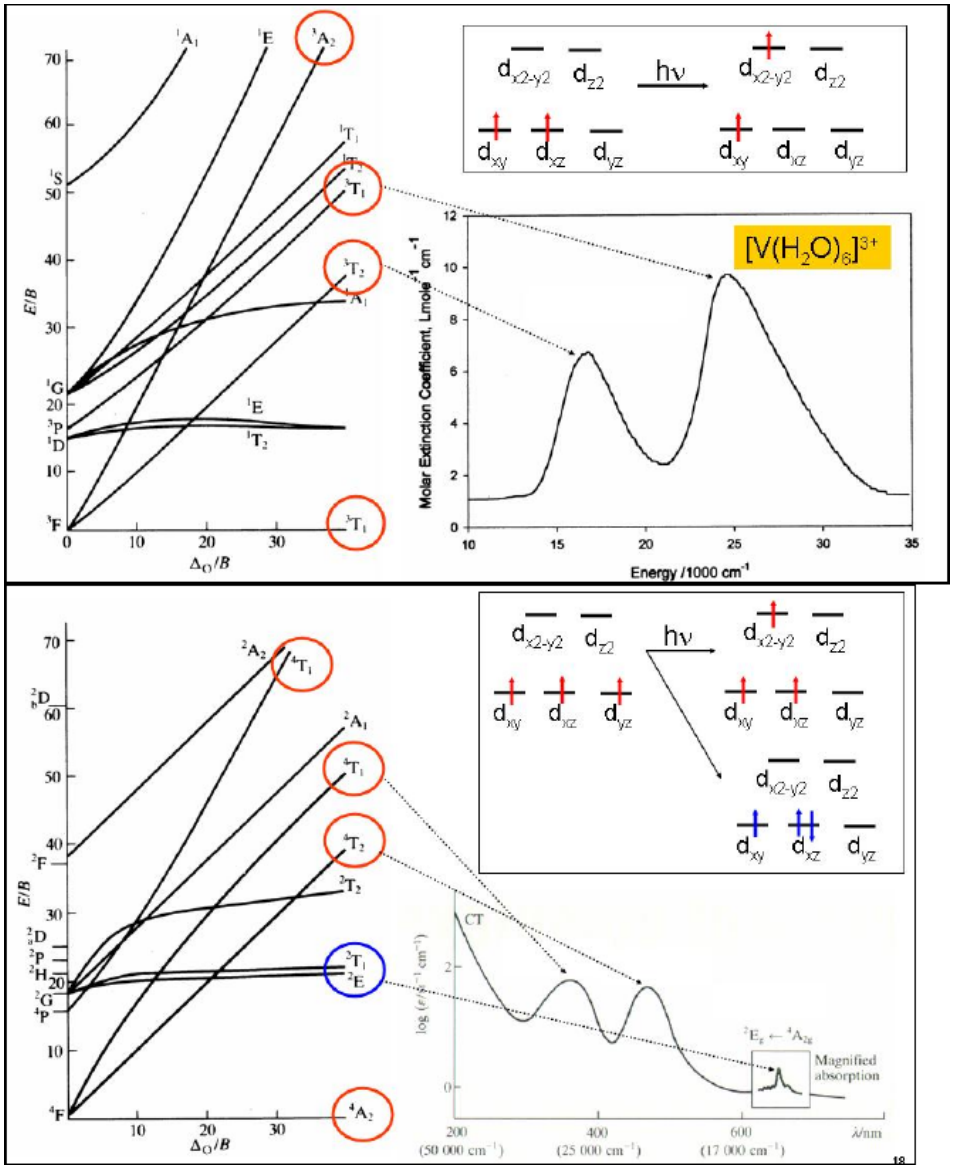

Figure 10: Example of a ligand field analysis for the d^2 and d^3 configurations on the basis of Tanabe-Sugano diagrams.

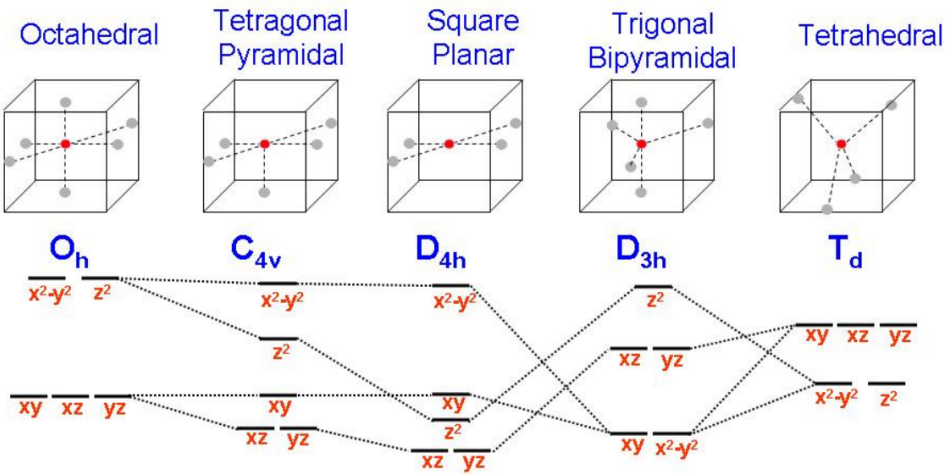

Figure 11: Orbital splitting patterns in different coordination geometries.

and, consequently, the coordination geometry can be inferred from a proper analysis of the absorption spectra and other optical techniques that probe the same transitions.

Inadequacy of the Ligand Field Theory: Covalency and the Nephelauxetic Effect

There is very good evidence from spectroscopic measurements that LFT is an oversimplification. For example, consider the following EPR experiment:

The EPR spectrum of $[\mathrm{Cu(imidazole)}_4]^{2+}$ is shown in Figure 12, and is a typical square-planar d^9 coordination complex, like many others in coordination chemistry. According to Figure 11 the unpaired electron resides in a metal $d_{x^2-y^2}$ orbital. The interesting sharp features in the EPR spectrum actually represent hyperfine structure that arise from coupling of the unpaired electron to four equivalent nitrogen nuclei of the imidazole ligand. The origin of these signals can be validated in the following manner: nitrogen has two accessible isotopes, ^{14}N (the naturally occurring isotope and also most abundant) and ^{15}N. In addition ^{14}N has a nuclear spin ($I = 1$) and ^{15}N a nuclear spin ($I = 1/2$), while the nuclear g-value of ^{14}N is twice as large as that of ^{15}N. Thus, synthesis of the imidazole ligand with ^{14}N and ^{15}N will lead to precisely predictable changes in the EPR spectrum, and this is how the nature of the signals can be experimentally verified, without any doubt.

The hyperfine structure is a measure of the probability of finding the unpaired electron near the nucleus in question. But, there is a discrepancy between the predictions of LFT and the experimental observations. According to LFT, the singly occupied molecular orbital (SOMO) should be a pure metal d orbital, and have no probability of finding the electron at the nitrogen nucleus. The epr experiment shows a different result, which displays electron density near the nitrogen nucleus. It turns out that this experimental finding is readily explained on the basis of MO theory.

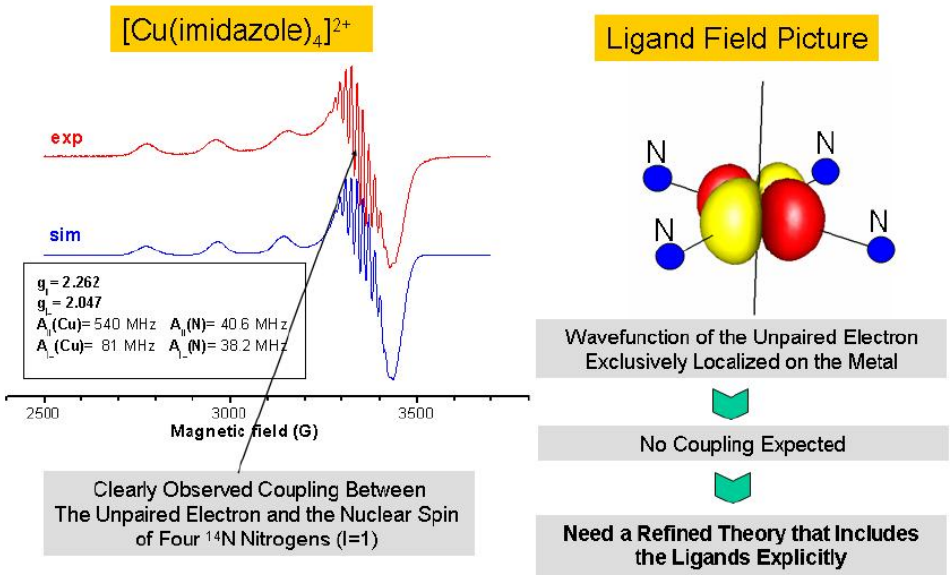

Figure 12: The EPR spectrum of $[Cu(imidazole)_4]^{2+}$ (left). On the right is the singly occupied orbital according to Ligand Field Theory. On this basis, the sharp features in the middle of the spectrum cannot be explained.

The shape of the SOMO is shown in Figure 13, and it is evident that the SOMO indeed has $d_{x^2-y^2}$ character on the central copper atom. However, the $d_{x^2-y^2}$ orbital is σ-antibonding with the coordinating imidazole-nitrogens. Thus, part of the unpaired spin-density is delocalized into these ligand atoms, and this accounts for the experimental observations. In fact, from the experimental data, one is able to make a semi-quantiative estimate of how much spin is required to be on the nitrogens in order to explain the experimental data. In the present case, this amounts to ∼60-65% spin population on the copper atom, with some ∼9-10% on each nitrogen.

The dilution of the metal orbitals with ligand character has in fact also been noted by the optical spectroscopists interested in LFT, who needed to account for electron-electron repulsions that were smaller than expected from atomic spectroscopy. They explained this finding by an increase of the size of the metal orbitals and called it the *nephelauxetic effect* (i.e. a cloud expanding effect). However, a much more natural explanation is obtained in terms of MO theory. Mixing of ligand character into the metal orbitals is referred to as metal-ligand covalency, and the more covalent the metal-ligand bond, the more ligand character that is mixed into the metal-based MOs.

Molecular Orbitals of Octahedral Complexes

The discussion above raises the question of how the MO theory of coordination complexes works in general, and has been worked out in great detail in many textbooks, but a brief discussion will be provided here. A typical MO scheme for an ML_6 complex can be derived from extended Hückel calculations. Thus, one considers that ionization potentials of transi-

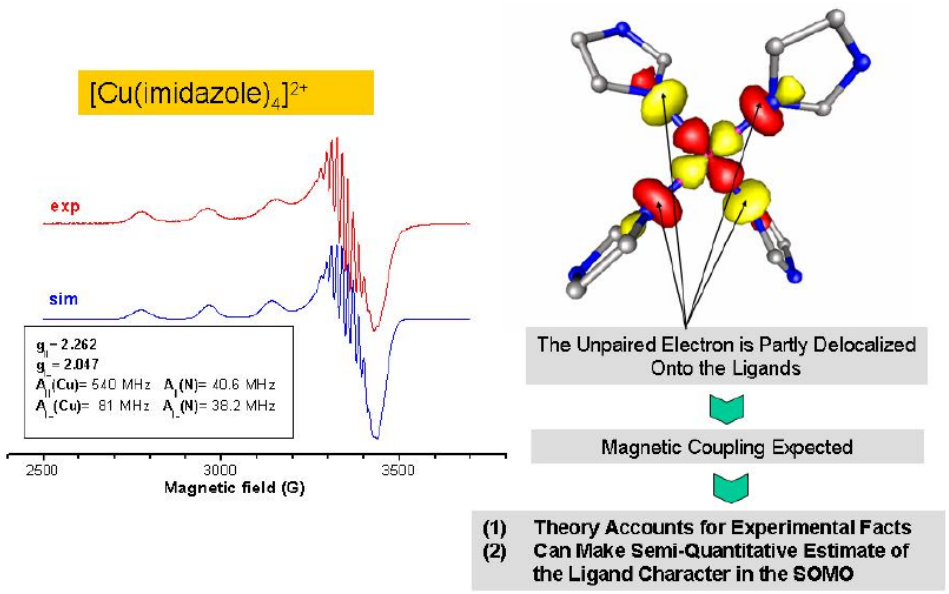

Figure 13: Interpretation of the EPR spectrum of $[\text{Cu(imidazole)}_4]^{2+}$ according to MO theory

tion metals are typically a few eV lower than those of main group atoms. Consequently, the metal orbitals nd, $(n+1)s$, and $(n+1)p$ to 0th order are at higher energy than the ligand s and p orbitals. Perturbation theory then tells us, that upon forming molecular orbitals from fragment orbitals of correct symmetry, the high-lying orbitals become destabilized and antibonding, and the lower lying orbitals become stabilized and bonding.

The smaller the energy gap between the mixing fragment orbitals, the stronger their interaction, the larger will be the admixture. Thus, the metal d-orbitals of Ligand Field Theory are the partially occupied antibonding orbitals that can be found in MO calculations on coordination compounds. Some typical bonding and antibonding components are shown in Figure 14.

It is evident that the metal-based t_{2g}-orbitals correspond to π-antibonding MOs while the metal-based e_g-orbitals correspond to σ-antibonding MOs. Since π-interactions are typically weaker than σ-interactions, this accounts for the energetic ordering of the two-sets of orbitals correctly predicted by LFT.

An interesting and subtle point is that this MO scheme cannot be derived from Hartree-Fock (HF) calculations. In HF calculations, the metal orbitals typically fall energetically below the ligand orbitals, but are still the first to be ionized. This arises because the electronic relaxation energy upon ionization is small for the ligand orbitals and very large for the metal orbitals. On the other hand, the extended Hückel like arguments give a somewhat correct picture of the ionization events in complexes, but the quantitative theory is more complicated. In extended Hückel and other semiempirical theories, the metal-ligand interaction is taken to be proportional to the overlap between the metal and ligand fragment orbitals. These interaction parameters are called resonance integrals.

It is also clear that the M-L bonding orbitals are always fully occupied, that the metal-based d-orbitals are usually partially occupied, and that there is a net transfer of charge from the

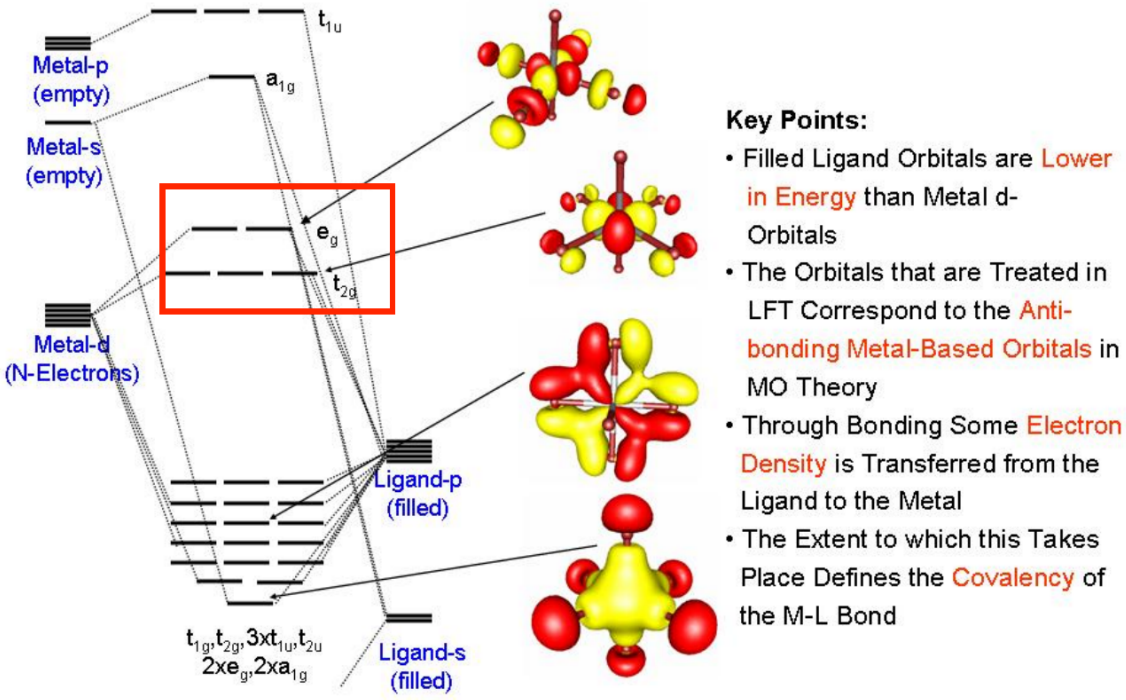

Figure 14: MOs of octahedral ML_6 complexes. The red box shows the five metal-based MOs that are the ones taken into account in ligand field theory.

ligand to the metal. Thus, in MO theory, one never finds partial charges that come close to the formal charges, as measured by the oxidation state. However, as long as the mixing between metal- and ligand-orbitals is not extremely excessive (e.g. exceeding 30%-40% ligand character on the metal orbitals), the concept of a d^n configuration that is so central to LFT still remains valid. But, one simply has to realize that the orbitals are partially delocalized onto the ligands. From this discussion, it also becomes evident that it does not make sense to try to compare the partial charges from a MO calculation to the charge implied by the formal oxidation state.

π-Bonding and π-Backbonding

There is one important class of ligands that do not perfectly correspond to the discussion given above. These are ligands that have low-lying empty π^* orbitals, or filled donor p or π orbitals, which can interact with the metal-based t_{2g} orbitals to form π-bonding and π-antibonding orbitals.

However, in this case, the nature of the donor and acceptor orbitals is reversed compared to the standard σ-donor ligands discussed above. Thus, the interaction of empty π^* orbitals on a ligand ***stabilizes*** the metal t_{2g} orbitals and become bonding. Furthermore, occupation of these orbitals leads to a backflow of charge from the metal to the ligand this type of bonding is therefore called backbonding. On the other hand, filled π or p orbitals on a ligand ***destabilize*** the metal t_{2g} orbitals and become antibonding.

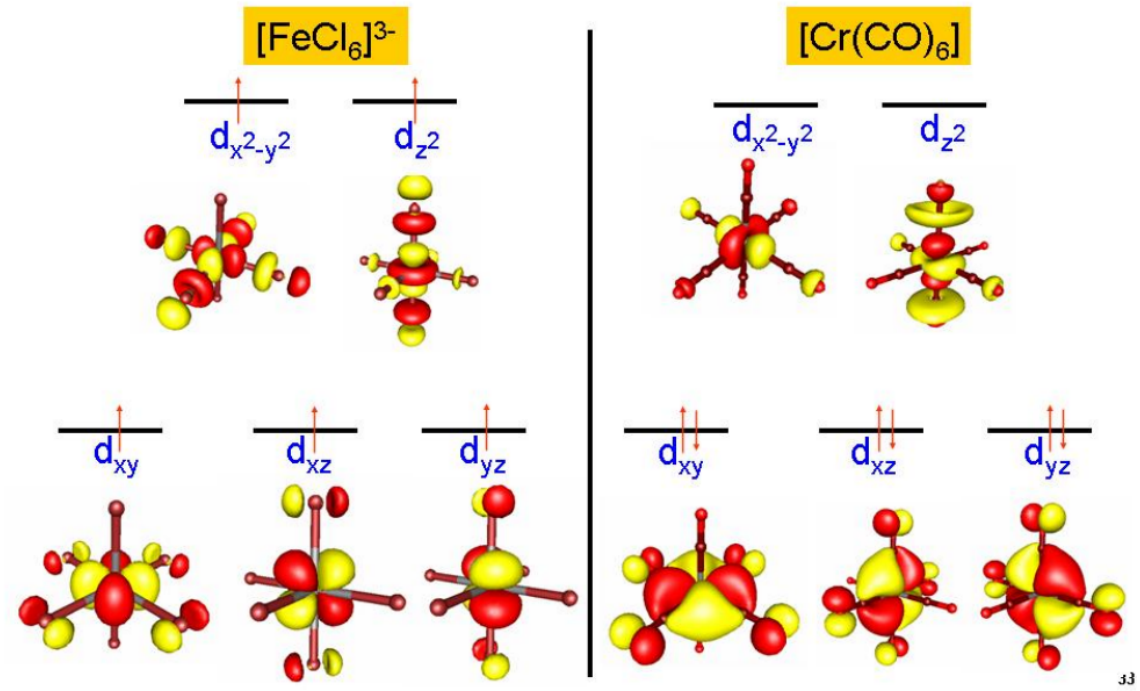

Figure 15: Orbitals in π-donor and π-acceptor complexes.

The effect is exemplified in Figure 15, where the standard π-donor complex $[FeCl_6]^{3-}$ (a high-spin d^5 complex) features metal t_{2g} based orbitals that are π-antibonding with filled Cl ligand p orbitals, while those of $[Cr(CO)_6]$ (a low-spin d^6 complex) are π-bonding with CO π^* orbitals. The effect of π-backbonding naturally is very pronounced on the ligand-field splitting. Thus, the metal t_{2g}-orbitals are stabilized through backbonding, the metal-e_g orbitals are destabilized due to σ-bonding, and the net effect is an increase in the ligand-field splitting. The opposite effect is of course true for standard π-donor complexes – the better the π-bond between the metal and the ligand, the smaller the ligand field splitting. As discussed earlier, the OH^- ligand is a weaker field donor than H_2O. Because of the negative charge on OH^-, the energy of p donor orbitals are raised becoming closer to the t_{2g} orbitals of the metal, leading to stronger a $\pi - d_\pi$ interaction and a concomitant narrowing the $t_{2g} - e_g$ splitting.

On this basis, a much more appealing interpretation of the spectrochemical series can be given as shown in Figure 16. Strong-field ligands are π-acceptor ligands, while weak-field ligands are good π-donor ligands. In the middle of the spectrochemical series are those ligands that do not have π-orbitals for either bonding or backbonding available, for example NH_3 or neutral aliphatic amines.

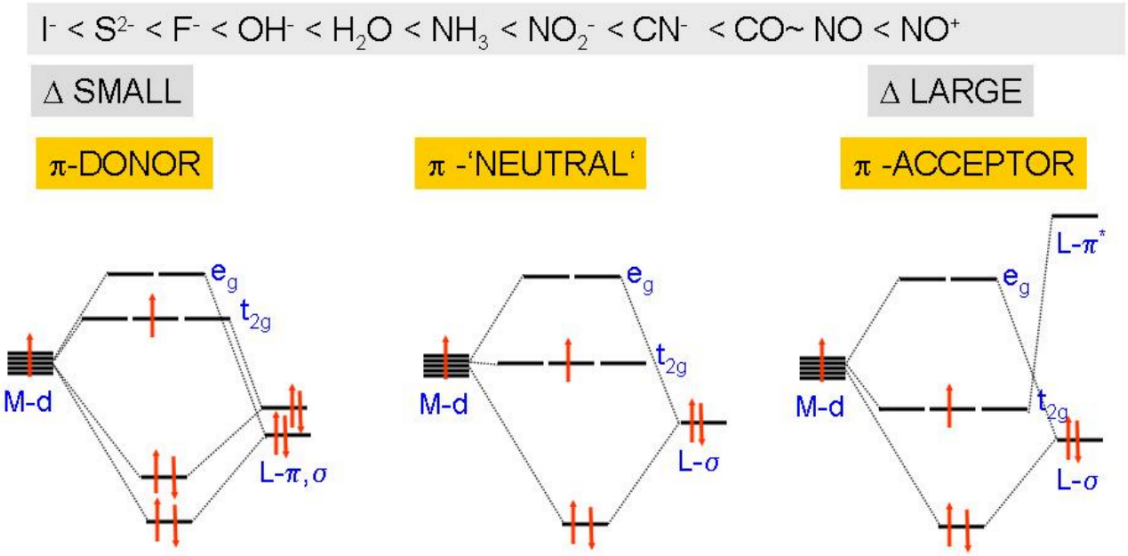

Figure 16: Interpretation of the Spectrochemical Series on the Basis of MO Theory.

General Comments for the Calculations

Below are several problems in computational coordination chemistry that are more or less representative of transition metal coordination chemistry.

In general very small basis sets (SV for the metal and the oxygens and STO-3G for the hydrogens) will be used in order to minimize calculation times. In practice, it is advisable to use at least polarized triple-ζ basis sets for the metals and at least polarized double-ζ basis sets for the ligands in order to obtain reliable results.

As a generic template for the calculations, approximately octahedral fragments with water ligands will be used. Appropriate metal-ligand bond distances are shown in Table 2 for M(II) and M(III) ions of the first transition row. The complexes studied will be of the form $[M(H_2O)_5X]^{n+}$ where M is a first-row transition ion and X is an additional ligand that will be varied in the course of the experiment. For X=H_2O, the highest possible symmetry that such complexes can assume is T_h which is another cubic group.

	Divalent	Trivalent
Ti	-	2.028
V	2.128	1.992
Cr	2.052	1.959
Mn	2.192	1.991
Fe	2.114	1.995
Co	2.106	1.873
Ni	2.061	-
Cu	1.964	-

Table 2: Bond distances (Angstrom) for divalent and trivalent hexaquo ions of the first transiton row.

The application of DFT to transition metal complexes is often successful but not without its pitfalls. One problem in the present case, where we deal with highly symmetric complexes, is that DFT applies only to orbitally nondegenerate ground states. For degenerate ground states, symmetry breakings occur which may lead to artifacts in the calculations.

In practice this is usually not such a strong limitation, since most systems of practical interest are not orbitally degenerate. Even those that are orbitally degenerate are Jahn-Teller active, and become orbitally nondegenerate upon distortion. In these exercises, the focus will be on d^n configurations with orbitally nondegenerate ground states.

Intersection of Ligand Field Theory and Density Functional Theory

1. Perform calculations for the $[Cr(H_2O)_6]^{3+}$ complex, and on other similar d^3 complexes, including $[V(H_2O)_6]^{2+}$, the hypothetical $[Ti(H_2O)_6]^{+}$, the d^8 system, $[Ni(H_2O)]^{2+}$, and hypothetical $[Cu(H_2O)_6]^{3+}$.

   Observe the results of the population analysis. How does the partial charge on the metal change? How does the spin-population at the metal change?

   Look at the occupancies of the metal d-orbitals. What does that say about $\sigma-$ and $\pi-$donation of the water ligands? How does it compare with the formal occupations? Compare the spin-populations of the d^3 and d^8 systems. What do you observe?

2. Calculate the first six ligand field excited states for the transition metal complexes given in Question 1 above, and determine Δ_0 and B from the computational results.

   The energies of the two transitions from LFT for both the d^3 and d^8 complexes, are given by:

d^3	d^8	Energy
$^4A_{2g} \rightarrow {}^4T_{2g}$	$^3A_{2g} \rightarrow {}^3T_{2g}$	$\Delta E = \Delta_0$
$^4A_{2g} \rightarrow {}^4T_{1g}$	$^3A_{2g} \rightarrow {}^3T_{1g}$	$\Delta E = \Delta_0 + 12$ B

   Thus, from the calculations, the values of 0 and B can easily be determined.

3. The ratio of $\frac{\text{B(complex)}}{\text{B(free ion)}}$ is known as the nephelauxetic ratio. Calculate the nephelauxetic ratios for the series of complexes given in Question 1 above.

   The Racah-parameters (B) of the free ions are: Cr^{3+}=950 cm^{-1}, Ti^{2+}=720 cm^{-1}, Ti^{+}=680 cm^{-1}, V^{2+}=765 cm^{-1}, V^{3+}=860 cm^{-1}, Ni^{2+}=1080 cm^{-1}, Ni^{+}=1040 cm^{-1} , Cu^{2+}=1240 cm^{-1}, Cu^{+}=1220 cm^{-1}, Cu^{3+}=1260 cm^{-1}.

   Are the nephelauxetic ratios larger or smaller than unity? Explain. Do the trends in nephelauxetic ratios make sense in terms of your chemical intuition?

   Will the nephelauxetic ratios depend on the nature of the metal, including the oxidation state and the ligand? Please explain your answer.

   What do you include with respect to the ability of TD-DFT to model the values Δ_0 and B correctly?

4. Study the dependence of Δ_0 and B on the metal-ligand distance of $[Cr(H_2O)_6]^{3+}$. Does the result match your expectation?

   Which power of the metal-ligand distance R do you expect Δ_0 to vary based on conventional ligand field arguments?

Positions of Ligand and d Orbitals in Transition Metal complexes

In many cases, it is difficult to unambiguously identify the metal based MOs. This is particularly so for later metals, higher oxidation states, and increasing numbers of unpaired

electrons. The reason is that higher oxidation states tend to stabilize the d-orbitals, and, consequently, move closer to the ligand orbitals. In addition, a large number of singly occupied orbitals that are mainly centered on the metal lead to a very large exchange stabilization which further suppresses the energies of the occupied spin-up orbitals.

As a consequence, metal-based MOs move down in energy near or below the ligand based orbitals. This effect is more pronounced as more Hartree-Fock exchange is present in the density functional, and is extremely strong for the Hartree-Fock method itself. Yet, the ligand field picture is not invalid but simply more difficult to recover from MO calculations.

One useful way to unravel the distinction between ligand and d orbital involves a localization procedure, followed by analysis and visualization of the localized orbitals (LCOs) composed of mainly metal character.

Localized orbitals never show a bond where there is none. Thus, if a bonding and an antibonding partner of a bond are both fully occupied, the localization procedure simply separates the two constituents into atomic or fragment orbitals. A bond remains only if the antibonding partner is in the virtual space. Thus, localization and orbital inspection is a good way to discuss the net bonding effects.

Another useful way to obtain a clearer discription of ligand and d orbital is through the calculation of Restricted Orbitals (QROs), where those that are singly occupied will correspond well with ligand field expectations and is another useful analysis tool.

1. Perform a calculation on $[Fe(H_2O)_6]^{3+}$ and inspect the canonical orbitals in both the spin-up and spin-down sets. Where are the metal orbitals? What is their composition? What are their energies? How would you interpret these results?

2. Localize the orbitals, and then visualize them.

   What does your result imply in terms of frontier molecular orbital theory? Where do you think will an electron go upon reduction of the complex to the ferrous form?

3. Obtain a set of QROs, and analyze their composition, and visualize them.

   Do these results with QROs lead to a better description for the ligand and d orbitals?

Covalencies of Metal Ligand Bonds

As mentioned in the introduction to this chapter, the coalvency of the metal ligand bonds is an important factor in determining the physical and reactive properties of transition metal complexes. Covalency here is defined as the ability of the metal and the ligand to share electrons. A quantitative measure for this is how much ligand character is mixed into the metal d-based orbitals, and vice versa.

The unitary invariance of the wavefunction (or Kohn-Sham determinant) with respect to rotations among occupied orbitals are not observables. However, it is chemically sensible to study the variations in metal-ligand bonding by looking at the metal-ligand bonding and antibonding orbitals.

Consider the $[M(H_2O)_6(X)]^{n+}$ complexes and vary X for fixed M and then M for fixed X, where X can be: CO, CN^-, NH_3, OH_2, O^{2-}, S^{2-}, F^-, Cl^-, Br^-, and I^-.

1. For the hypothetical complexes $[Cr(H_2O)_5(X)]^{3+}$, $[Cr(H_2O)_5(X^-)]^{2+}$, and $[Cr(H_2O)_5(X^{2-})]^+$, optimize the geometry of the complexes using the small basis set defined above.

   Calculate the energies of the system using the B3LYP functional in single point calculations, and include a water solvation model. Look at the metal-t_{2g} and metal-e_g derived orbitals.

   Discuss σ-bonding versus π-backbonding, and how it varies with the ligand. What changes are observed in the populations of the metal d-orbitals?

2. Analyze and visualize localized molecular orbitals.

   Localized orbitals never show a bond where there is none. Thus, if a bonding and an antibonding partner of a bond are both fully occupied, the localization procedure simply separates the two constituents into atomic or fragment orbitals. A bond remains only if the antibonding partner is in the virtual space. Thus, localization and orbital inspection is a good way to discuss the net bonding effects.

   What conclusions can be inferred about the nature of the bonds?

3. From the total energy calculations, compare the bond energy of the X ligand relative to the hexaquo complex. It will be necessary to run a geometry optimization plus energy for the free X ligands. How does the bond energy vary with the ligand and the oxidation state of the metal? Is it in accord with your chemical intuition?

4. Repeat the calculations for fixed ligands with a lower-valent metal, for example, the low-spin configuration ($S = 0$) of Fe(II). How does the ability of the metal for backbonding change?

Organometallics

The field or organometallic chemistry is quite important because versatile and powerful catalysts can be designed on the basis of such complexes. Here, a brief look is taken at an iconic organometallic compound, ferrocene, $Fe(cp)_2$.

1. Run a single point calculation on $Fe(cp)_2$ using the BP86 functional and the small basis set used throughout these exercises.

   Analyze the electronic structure of the complex using orbitals and populations. What is the nature of the metal ligand bond?

2. Perform a calculation on the free cyclopentadienyl ligand and determine the fragment orbitals that contribute most to the bonding. Construct a fragment orbital interaction diagram.

3. Use the BHLYP functional to calculate the first 15 electronically excited states.

   What is the nature of these transitions, and compare the transition energies with $d-d$ transition energies of the hexaquo complexes that were studied above. What do you observe? What is the interpretation of what is observed? Determine the dominant donor and acceptor orbital pairs. Work out the symmetry of the final electronic states. Determine the selection rules for the electric dipole and magnetic dipole transitions.

Potential Energy Scan of $[CuCl_4]^{2-}$

The complex ion $[CuCl_4]^{2-}$ is known to exist in different crystals with varying counterions. While Cu(II) normally prefers a square planar coordination, this ion is found in various forms ranging from square-planar to almost tetrahedral.

The energy associated with this distortion will be calculated. A rigid potential energy surface, beginning with a square planar and ending with a tetrahedral structure, is performed by defining a Cl-Cu-Cl distortion angle which varies from 0 to a final value of (180-109.4712)/2.

1. Perform the potential energy scan, convert the energies to relative energies in kcal/mol, and plot the resulting potential energy surface.

   A larger number of steps can be employed in order to obtain a more smooth looking surface.

   Where do you find the minimum? Does it require a lot of energy to distort the molecule?

2. Determine the change in electronic structure by examining two or three points along the surface.

   Examine the orbitals and populations.

3. Calculate the first four ligand field excited states. Do you think that spectroscopy will be a useful indicator of the coordination geometry?

   This calculation represents one of the cases where TD-DFT with normal GGA functionals like BP86 fails badly, and predicts LMCT states where there should be d-d excitations (in the region below $\sim$15000 cm^{-1}). The calculation should, instead, be performed with a functional that includes more HF exchange. BHLYP is recommended which introduces as much as 50% HF exchange. It may also be necessary to calculate more than the desired four ligand field states in order to capture the states of interest, since they do not come in order of increasing orbital energy difference. To be on the safe side, a calculation with 25 states should be sufficient. Observe the assignment of the transitions and see where the occupied metal orbitals are in the spin down set.

   Draw an MO diagram.

Reactivity: Powerful Oxidants

The interesting species $[Fe(IV)O(H_2O)_5]^{2+}$ has been synthesized and will be studied in section. It is a simple model for related Fe(IV)-oxo species that are of much relevance to

chemistry and biochemistry since they are powerful oxidants. The most intensely studied system is Cytochrome P450 which features a very complicated electronic structure. The active species involves an iron-oxo group coupled to a porphyrin radical.

Some aspects of structure, bonding and energetics of such species will be studied.

1. Firstly, determine which spin state is the lowest one for this system, i.e. $S = 1$ or 2. Optimize the structure of the species. Repeat the optimization for the low-spin state.

2. Analyze the electronic structure of both species.

   What are the electron configurations in the two states? How did the structure change?

   How did the changes in the structure reflect the different electronic configurations? Is the oxo-group strongly affected by the change in spin state?

   More interestingly for the synthetically oriented chemists is the question of how to choose a ligand which will force the system to adopt either one or the other ground state?

3. Recalculate the energies at the optimized geometries using the B3LYP functional.

   For more quantative results, is necessary to perform the calculation with much larger basis sets: geometry optimization with TZVP basis set, and final energy calculation with TZVPP basis set. This will not be done here, in order to keep the computation times short. In a serious study, one would also want to evaluate the zero-point energy and thermal contributions to the energy differences.

   What is the energy difference between the two states? Could either be the ground state?

4. Study the hydrogen atom abstraction reaction:

$$[FeO(H_2O)_5]^{2+} + CH_4 \rightarrow [Fe(OH)(H_2O)_5]^{2+} + CH_3$$

   - Optimize the structures of the reactants and products (assume $S = 5/2$).
   - Recalculate the energies using B3LYP single point calculations.
   - Is the reaction predicted to be feasible? If not, would this molecule be able to oxidize weaker C-H bonds such as that of toluene?
   - Analyze the structure of the reaction product. What are the major geometric changes? What are the electronic changes brought about by protonating the oxo group and reducing the metal? What happens to the Fe−O bond and covalency?

5. Compare the capability of this iron-oxo species to two other systems: OH· radical and the well-known species, $[VO(H_2O)_5]^{2+}$ which will require another set of geometry optimizations.

Unusual Bonds and Coordinated Radicals: Iron-Nitrosyls

Questions of structure and bonding can become quite complicated when the oxidation state of the ligand becomes ambiguous. A famous example are transition metal nitrosyls. Here the NO ligand is believed to be able to coordinate as NO^-(S=1), NO^-(S=0), NO·(S=1/2) and NO^+(S=0) depending on the metal and formal oxidation state, and the remaining ligand set. Since the interpretation is often ambiguous, Enemark and Feltham have invented the $\{MNO\}^x$ notation, where x is the number of metal-d plus NO-π^* electrons. Thus, the reaction of Fe(II) with NO yields a $\{FeNO\}^7$ complex.

The $[Fe(H_2O)_5(NO)]^{3+}$ complex ion will be studied, and is well-known to every chemist as the brown ring complex in analytic chemistry, but has a quite complicated electronic structure.

1. Optimize the geometries of $[Fe(III)(H_2O)_5(NO^+)]^{3+}$ ($S = 5/2$), $[Fe(II)(H_2O)_5(NO\cdot)]^{3+}$ ($S = 3/2$), and $[Fe(I)(H_2O)_5(NO^-)]^{3+}$ ($S = 1$).

   Use initial parameters with an Fe−NO bond distance of 1.76 Å, Fe−O bonds of 2.12 Å, an N−O distance of 1.2 Å, and a Fe−N−O bond angle of 170°.

   How does the N−O distance change with oxidation state? How does the Fe−N distance change? What do these values mean with respect to the oxidation state of the ligand?

   Compare these values to the free $N-O^+$, N−O·, and $N-O^-$ bond distances.

   Do you observe trans effects?

2. Analyze the bonding using orbitals, spin populations, electron populations, and bond orders.

   An additional analysis tool that can be used here involves unrestricted corresponding orbitals (UCOs) which consists of spatial overlaps of spin-up and spin-down orbitals. Overlaps close to zero, or at least significantly smaller than one, indicate a spin coupled system. In this case, the spin-expectation value $< S^2 >$ will significantly deviate from $S(S+1)$ which can be found in the output.

   What is your interpretation if such a spin coupled system is found here? Examine the UCOs, and observe which orbitals are spin coupled (if any).

   What is your best description of the electronic structure in terms of d^n configurations, and is the d^n designation sensible in this case?

   Analyze the composition of the UCOs

3. Are there alternative spin states, and are they lower in energy than the those that were just calculated?

High-Spin/Low-Spin and Spin-Crossover

An important field of investigation deals with transition metal complexes that have two thermally accessible spin states. Such complexes are spin-crossover systems and feature ligand field strengths that are just on the border of the strong- and the weak-field parts of

the Tanabe-Sugano diagram. This case is particularly frequently met in Fe(II) complexes, where the ${}^5T_{2g} - (t_{2g})^4(e_g)^2$ and ${}^1A_{1g} - (t_{2g})^6(e_g)^0$ states are part of the spin-crossover system. An accurate calculation of the energy difference between these two states is obviously very complicated as one needs to reach an accuracy that is on the order of the thermal energy ($\sim$200 cm^{-1}).

Moreover, the spin-crossover is frequently driven by cooperative and entropic effects which are particularly difficult to model with quantum chemical methods. Nevertheless, it is especially difficult problem for DFT methods to make predictions that are within a reasonable range, since the results of various functionals were found to differ by very large margins.

SCF convergence may be somewhat challenging for this complex, since the $(t_{2g})^4(e_g)^2$ configuration is almost orbitally degenerate, and the orbital energy difference between the spin-down HOMO and the spin-down LUMO is only $\sim$0.2 eV. The calculations with the hybrid functionals are more likely to converge better and might be taken as input for the calculations that do not involve HF exchange.

In the present work, a very simple model is used instead of the frequently studied spin-crossover complex, $[Fe(phen)_2(NCS)_2]$. The phen ligands are substituted by NH_3 ligands yielding the $[Fe(NH_3)_4(NCS)_2]$ so that computational time can be reduced .

1. Inspect the calculations for the two complexes, and determine the main difference between the high-spin and low-spin geometries. What is the relationship between the geometric and electronic structures?

2. Perform single point calculations on both structures using the UHF method, and the BHLYP, B3LYP, BLYP, BP96 and LSD functionals. Compare your results using the standard small basis set.

   To which extent can one want to rely on DFT methods to predict spin state energetics? Is the Hartree-Fock method an attractive alternative?

Exchange Coupling Between Transition Metal Ions

A final important subject involves is the magnetic coupling between open-shell transition metal ions. There is a large class of multinuclear transition metal systems, with constituent ions, that have unpaired electrons based on their electron count. These unpaired electrons on different sites typically couple weakly to produce a ladder of spin states, which may be described phenomenologically by a so-called Heisenberg Hamiltonian that has the form $-2J * S_A * S_B$ where S_A and S_B are the spin-operators for sites A and B, and J is the exchange coupling constant. If J is negative, low-spin states are preferred, and the system is said to be antiferromagnetically coupled. A positive J refers to ferromagnetic coupling. The ordering of spin-states has important implications for many branches of chemistry and physics.

It is important to understand that this magnetic coupling is not related to experimental magnetic interactions. The origin of the exchange coupling is purely electrostatic in origin and is intimately associated with the antisymmetry of the N-particle wavefunction. There

is no exchange interaction in nature. What is described as exchange interaction, is merely the combined action of antisymmetry and electron-electron repulsion.

The accurate calculation of exchange coupling constants is quite challenging. In principle, multi-determinantl methods are required to provide a proper description of the low-spin states. The values of J are on the order of a few dozen to a few hundred wavenumbers. Thus, one has to calculate small differences between large numbers to high accuracy which is quite difficult.

The multi-determinant (not to be confused with multi-configurational) nature of the low-spin states would seem to invalidate DFT methods, which are based on a single determinant. However, the situation is can be managable, if some precaution is taken. Consider, for example, the case of two interacting Cu(II) ions, where both Cu ions are d^9 systems, and singlet and triplet states arise. The triplet state is straightforward to calculate with standard DFT methods, but the singlet state is more difficult to obtain.

The best way to approach the problem in DFT is to generate a so-called broken-symmetry (i.e. broken spin symmetry) solution in which one-electron localizes with spin-up on one site and another one with spin-down on the second site. This does not represent a correct singlet wavefunction, but merely a determinant with $M_S = 0$. Nevertheless, the physics of weakly interacting electrons is basically correctly described. Together with some approximate formalisms, it is possible to extract a value for J from a high-spin and a broken symmetry calculation.

The series of bis–hydroxy–bridged Cu(II)–dimers which represents a classical case of magneto-structural correlations will be studied. It has been shown experimentally, that a switch between ferromagnetic and antiferromagnetic coupling occurs as a function of bridging angle. The critical angle is found somewhere around 97°. A calculation can be performed to determine whether this result can be qualitatively reproduced.

1. Vary the angle, α, and search in the output for the predicted exchange coupling constant, and plots the values as a function of angle, α.

   Observe whether a change from $J < 0$ to $J > 0$ can be detected.